Conversion-Type Fluoride Cathodes: Current State of the Art

Lorenz F. Olbrich[a,*], Albert W. Xiao[a,*], Mauro Pasta[a,**]

[a] *Department of Materials, University of Oxford, Parks Road, Oxford OX1 3PH, United Kingdom*

Abstract

Conversion-type transition metal fluoride cathodes offer a 200% to 300% higher theoretical energy density limit than state of the art intercalation cathodes. Recent publications have reshaped our understanding of the reaction mechanism in these materials. Herein we review recent reports highlighting how active material dissolution, particle fusing, electrolyte consumption, and the resultant capacity fade can be mitigated by rational electrolyte design. Recent work has established the possibility of high discharge rate in transition metal fluorides at significant active material mass fraction; we examine the relationship between rate capability and active material fraction. Tuning transition metal fluoride chemistry via cation and anion substitution has demonstrated potential to improve its electrochemical properties. A brief techno-economic analysis is presented to highlight the practical advantages of different transition metal chemistries.

Keywords: Transition metal fluoride cathodes, conversion reaction, high energy density batteries, techno-economics, rate capability, electrolyte design

1. Introduction

Concerted measures on reducing greenhouse gas emissions are required to oppose ongoing climate change. Enabled by lithium-ion batteries (LIBs), the electrification of the automotive industry is progressing rapidly. [1] State of the art LIBs utilize open-framework transition metal cathodes which intercalate Li-ions into a limited number of interstitial sites within the stable host lattice. This storage mechanism imposes an upper physico-chemical limit for lithium storage (or charge storage), rendering such technologies unsuitable for applications that require even higher gravimetric energy densities, such as electric passenger aircraft. [2, 3]. Transition metal fluoride (TMF) cathodes, on the other hand, can store multiple Li-ions per metal center due to a multi-electron conversion reaction and hence offer a 200% to 300% increase in theoretical energy density if high redox potential metals are employed (Fe, Co, Ni, Cu). [4] In addition, the low cost per kilowatt-hour and environmentally benign properties of Cu and Fe make TMFs a promising class of next generation cathode materials for high energy density applications. [5, 6]

Unfortunately, TMF cathodes suffer from poor ionic and electronic conductivity due to a large bandgap induced by the ionic character of the TM-fluoride bond. [7] The initial cycling performance of TMF cathodes reported from 2003 onward by Badway and Li *et al.* exhibited short cycle-lives, sluggish kinetics, and a significant hysteresis which was ascribed to the insulating nature of TMFs and structural rearrangement required for the conversion reaction. [8, 7, 9] Despite these inherent obstacles, a considerable improvement in performance was achieved in the following 15 years through a variety of cathode engineering techniques, including utilization of various carbon composites, cation and anion substitution, and nanostructuring. [10, 11, 12, 13, 14, 15]

On the other hand, the mechanistic understanding of the conversion reaction evolved concurrently in a rather disconnected fashion. The most widely studied compound is FeF_x (x = 2, 3), often used as a prototypical model for other TMFs. A discussion on the symmetry of phase evolution, the presence of intermediate phases, and the nature of morphological transformations upon lithiation and delithiation ignited the scientific literature. The most widely accepted theory described a three phase direct conversion of FeF_2 to Fe and LiF. In the case of FeF_3, an initial reduction via the insertion of Li ions forms $Li_xFe_yF_z$ intermediate phases and FeF_2, followed by direct conversion to LiF and metallic iron. [8, 16, 7, 17, 18, 19, 20, 21, 22, 23, 24] However, in the last three years alone, the understanding of the conversion mechanism has changed drastically. In 2018, Karki *et al.* first suggested that FeF_2 conversion is topotactic in nature. [25] Subsequently, Xiao *et al.* demonstrated that the fluoride anion sublattice acts as a stable host enabling the topotactic transformation between LiF, FeF_2 and intermediate fluoride phases. [26] Very recently Hua *et al.* provided some additional evidence corroborating the role of the fluoride sublattice and elucidating the crystallographic characteristics of occurring intermediate phases in FeF_3 reduction. [27]

In light of this new mechanistic understanding, we will review the most recent developments on the electrochemical performance of transition metal fluorides, and pro-

*The authors contributed equally to this work

**Corresponding author, mauro.pasta@materials.ox.ac.uk

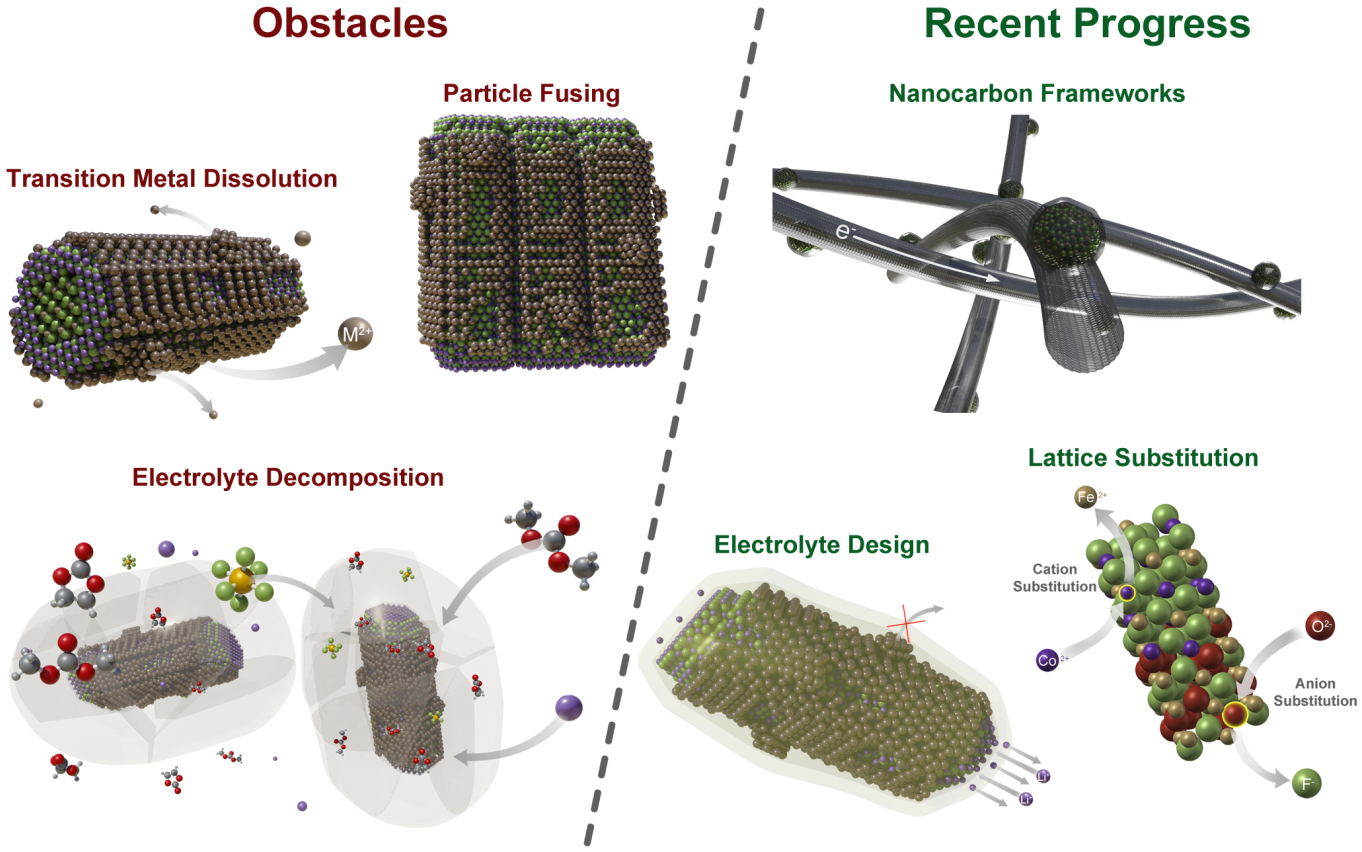

Figure 1: Bottlenecks and recent developments in the field of TMF cathodes. Capacity fade and high overpotentials in transition metal fluoride cathodes can be caused by active material dissolution, particle fusing, and continuous electrolyte consumption. Recent developments demonstrated successful mitigation thereof by rational electrolyte design, carbon supports, and metal-anion concerted doping.

vide a framework for further improvement of these battery chemistries. The impact of the electrolyte on cycle life, realistic prospects for rate capability, and utility of the lesser-studied transition metal fluoride compositions and their realistic energy densities will be discussed herein.

2. Improving Cycle Life Through Electrolyte Design

In general, TMF cathodes suffer from three major failure mechanism as illustrated in Figure 1. Active materials dissolution is reported for all transition metals of interest and is exacerbated by metallic phase segregation to the particle surface. [5, 6, 26] In addition, continuous electrolyte decomposition enabled by a low cut off potential (commonly set at around 1.2 V vs Li^+/Li) which is required for a complete transition metal reduction, can lead to the formation of a steadily growing cathode electrolyte interphace (CEI) and an accompanying rise in electrode and ohmic impedance. [28, 26] More importantly, CEI formation is further facilitated by the catalytic activity of the metal phase formed during discharge. [5] Lastly, ionic and electronic conductivity can diminish due to structural disintegration (loss of contact to current collector) or particle fusing. Fusing can substantially increase particle sizes beyond the diffusion lengths of conversion reactants which leads to the formation of isolated and unconverted material. [29, 6, 26] Rational electrolyte design can provide a pathway to tackle all of these as research from the last few years has shown.

Gu *et al.* described the benefits of using a 4.6 M lithium bis(fluorosulfonyl)imide (LiFSI) in dimethoxyethane (DME) electrolyte combined with a FeF_2 carbon nanocomposite. Cyclic voltametry, postmortem X-ray photo electronspectroscopy (XPS) and energy dispersive X-ray spectroscopy (EDS) indicated the formation of a stable passivation layer which prevented iron dissolution. At the same time the expected capacity fade within the first 20 cycles was drastically reduced. The best performing cell retained 80% discharge capacity after 1000 cycles. [30] In a subsequent publication the same group showed nearly complete capacity retention of more than 500 $mA\,h\,g^{-1}$ for 400 cycles using FeF_3 particles embedded on a carbon nanofiber (CNF) network in the same electrolyte. [31] Zhao *et al.* described a synergistic double protection layer effect by adding lithium bis(oxalato)borate salt to different organic electrolytes in conjunction with Al_2O_3 coated FeF_3 cath-

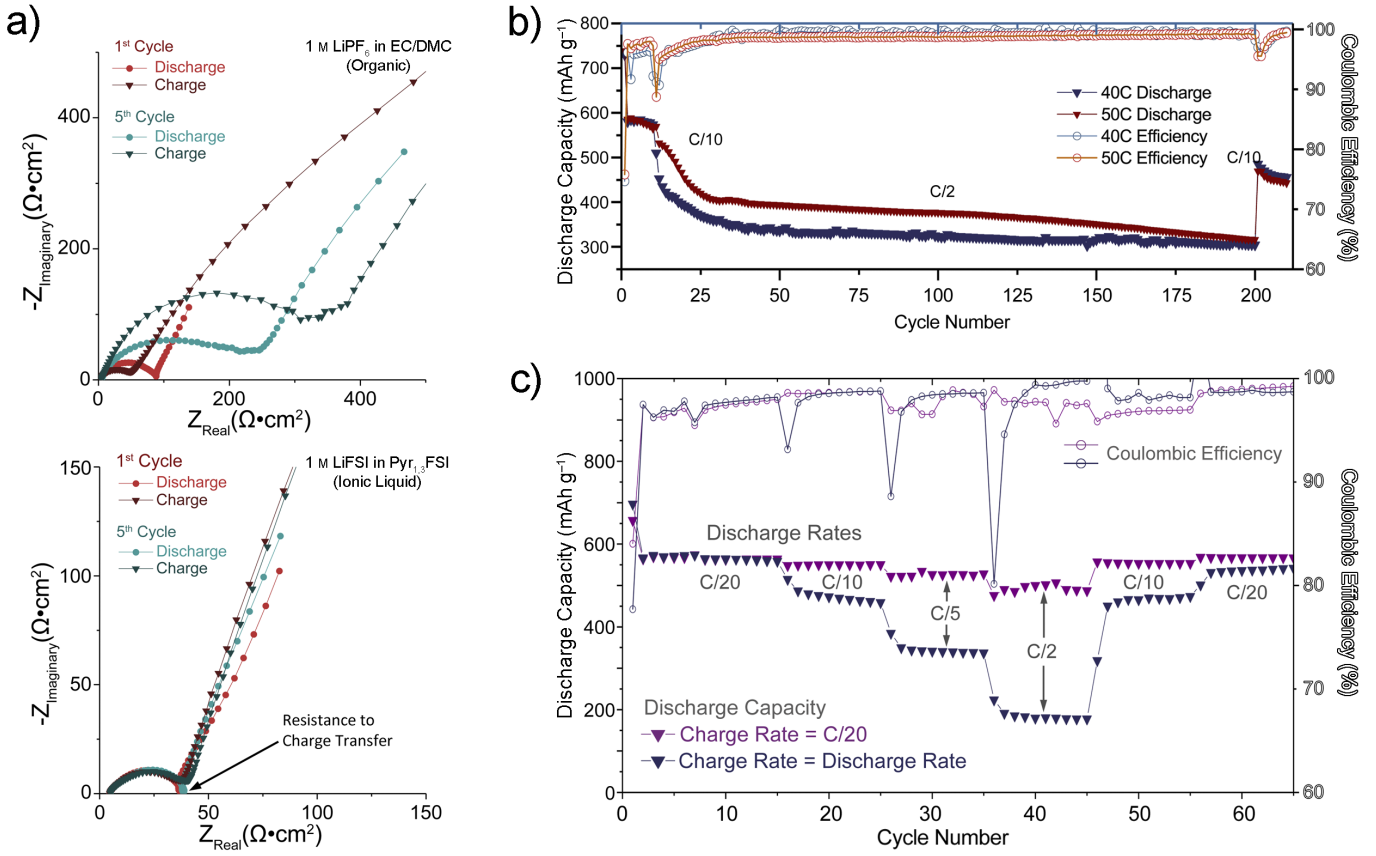

Figure 2: Electrochemical characteristics of FeF_2 reprinted with permission from [26]. **a**, Nyquist electrochemical impedance plots showing the difference in the magnitude and evolution of charge transfer resistance between an unstable electrolyte (1 M $LiPF_6$ in EC/DMC) and a stable electrolyte (1 M LiFSI in $Pyr_{1,3}FSI$). **b**, Plot of discharge capacity and coulombic efficiency vs. cycle number for FeF_2 electrodes at 40 °C and 50 °C showing stable cycling at elevated temperatures in an ionic liquid electrolyte. **c**, Plot of discharge capacity and coulombic efficiency vs. cycle number for FeF_2 electrodes cycled at various current densities. The dark purple plot shows cycling at equal charge and discharge rates. The light purple plot demonstrates the inherent discharge rate capability of the material when a slow charging rate (C/20) is applied to recover the full capacity.

ode particles. The CEI contained lithium oxalate and B-F bonds which successfully prevented iron dissolution and increased the capacity retention after 300 cycles from around 60% to 90%. [32]

Huang *et al.* studied the impact of organic electrolyte compositions on FeF_2 cycling in more detail. [28] They found that LiFSI fails to prevent cathode dissolution when dissolved in a fluoroethylene carbonate/ethyl-methyl carbonate (FEC/EMC) mixture contrary to an LiFSI DME solution. The authors rationalized this by the electrochemical instability of FEC which, when combined with LiFSI, can form an excessive CEI leading to cathode polarization. In contrast, the more electrochemically stable LiTFSI salt, showed superior performance when dissolved in FEC-EMC. In general, a thin uniform CEI was determined to be most beneficial for capacity retention. A new approach was reported by Huang *et al.* in 2019. FeF_2 was deposited on a carbon nanotube (CNT) network and infiltrated by a polymeric electrolyte. [33] The cathode exhibited a dense uniform distribution of FeF_2 which enabled acceptable ionic and electronic conductivity and an increased ductility. The all-solid-state cell operated at 50 °C and showed a discharge capacity of 450 mA h g^{-1} for over 100 cycles and almost complete capacity retention over 300 cycles, albeit at more limited cycling rates. Post-mortem analysis revealed the formation of a 6 nm-thin, stable CEI, which most likely originates from decomposition of the polymer and prevents cathode dissolution.

Xiao *et al.* reported multiple benefits of using LiFSI dissolved in an ionic liquid electrolyte (IL) with monodisperse FeF_2 nanorods. [26] In contrast to an organic electrolyte (LP30), which lead to cell degradation within the first 20 cycles, the IL ($Pyr_{1,3}FSI$) electrolyte enabled an unprecedented near-theoretical capacity retention (571 mA h g^{-1}) throughout the first 50 cycles and stable operation for over 200 cycles at 50 °C. Electrochemical impedance spectroscopy (EIS) revealed a constant charge transfer resistance during the initial five cycles and a minor increase thereafter which was in stark contrast to a rapid impedance rise observed in the organic electrolyte

(Figure 2a). Furthermore, XPS and TEM analysis indicated a high inorganic content in the 10 nm thick FSI^--derived CEI. Since no iron was detected on the counter electrode in postmortem XPS, it was concluded that iron dissolution was successfully hindered. Interestingly, the nanorods did not fuse and remained monodisperse during operation, which might be explained by the electrostatic interaction between the IL and FeF_2, and thus facilitated a high capacity retention (Figure 2b).

FSI^- anions are often implicated in the formation of a robust solid electrolyte interface (SEI) on lithium metal anodes, which improves their cycling stability. [34] As recent publications indicate, FSI^- anions also support the formation of a stable CEI on TMFs in either highly concentrated solutions (*e.g.* 4.6 M LiFSI in DME) or specific solvents (*e.g.* in DME or $Pyr_{1,3}FSI$). [30, 31, 28, 26] Since the CEI is formed during discharge (*i.e.* lithiation), the species solvating Li^+ have a significant impact on its structure and physical properties. [35, 36] In carbonate electrolytes FSI^- is generally reported to enter the solvation sheath of Li^+ only at very high LiFSI concentrations. [37, 38] In contrast, when employing weakly solvating electrolytes such as DME, FSI^- readily contributes to Li^+ solvation at more moderate concentrations. [39]. Hence, electrolyte design aiming for a FSI^- derived CEI should consider its solvating power and salt concentrations carefully.

3. A Realistic Look at Rate Capability

As discussed in section 1, TMFs are conversion type cathodes with intrinsically low electrical conductivity. As a consequence, higher charging/discharging rates are particularly plagued by high overpotentials or even complete cell failure. The most common techniques to overcome this hurdle use excessive amounts of conductive additives, often in the form of nanostructured carbon composites. For example, using the FeF_3 CNF composite mentioned in section 2, Fu *et al.* demonstrated the highest rate capability for FeF_3 systems, with a stable discharge capacity retention of $285\,mA\,h\,g^{-1}$ at $1000\,mA\,g^{-1}$. [31] The free standing CNFs prevent coarsening of the FeF_3 nanoparticles and the consequent formation of "dead material" and further enhance electronic conductivity enabling fast discharge rates. The best performing composite contains 56wt% active material (no additional binder and carbon required) which is still higher compared to other publication with similar carbon architectures. [33, 43, 40, 53, 49, 45]

Another approach was published by Li *et al.* based on a hetero-nanostructure of lithiated TiO_2 and FeOF combined with a CNT network. [48] TiO_2 becomes electronically conductive upon lithiation, which when combined with the CNT reduces the charge transfer impedance in the compound as evident from their EIS data. TiO_2 also provides reversible Li storage capacity and can act as mechanical confinement. Although discharge capacities of around $165\,mA\,h\,g^{-1}$ at $500\,mA\,g^{-1}$ are lower than in other reports, the group does achieve a stable areal capacity of $1.74\,mA\,h\,cm^{-2}$ for 300 cycles (at $100\,mA\,g^{-1}$). Thermogravimetric analysis indicates an active materials (FeOF and TiO_2) weight content of around 50 wt%.

In general, carbon architectures do not only enable higher cycling rates but also represent a successful strategy to mitigate particle fusing and can potentially be used to stabilize nanoparticles with an artificial CEI layer. [13] Unfortunately, carbon additives in excess of 40 wt% would reduce the specific energy of an FeF_2-lithium cell below that of commercial intercalation-based cells, and indeed an active material mass fraction of less that 70% would render most transition metal fluoride chemistries noncompetitive with next-generation, intercalation-based lithium-metal cells as discussed in more detail in section 4 and the supplementary information. The high rate performance comparison shown in Figure 3 illustrates the trade-off between areal capacity and discharge currents and their corresponding discharge capacities as a function of active material loading.

However, with the novel description of the topotactic reaction mechanism within a stable fluoride sublattice in FeF_x, the discharge rate appears to be not as intrinsically slow as initially assumed. Xiao *et al.* showed that the charging process is limited by the diffusion rate of iron across a high energy Fe-LiF interface whereas discharging is limited by Li^+ diffusion along open channels in the $\langle 1\,0\,0\rangle_{FeF_2}$ direction, which is inherently faster. Hence, by maintaining a slow charging rate to reach the full capacity ($28.6\,mA\,g^{-1}$), unprecedented high discharge capacities of $500\,mA\,h\,g^{-1}$ at $285.5\,mA\,g^{-1}$ could be demonstrated while maintaining an active material loading of 70wt% and an areal capacity of around $600\,\mu A\,h\,cm^{-2}$ (Figure 2c).

Another potential strategy for mitigating sluggish reaction kinetics and thus improving the rate capability of TMFs is operation at elevated temperatures. Unfortunately, cathode dissolution and electrolyte decomposition are accelerated as well and very little is known about degradation processes at higher temperatures. [58] Stable cycling has only been shown up to 50 °C. [26, 28] A recent mechanistic study on Fe^{3+}/Fe^{2+} redox reaction at 90 °C, indicates the difficulties of capacity retention at such high temperatures. [59]

4. Beyond Iron Fluorides

In Figure 4 we present a simplified techno-economic model for the later 3d TMF-lithium chemistries to establish a reasonable perspective on achievable energy densities and associated costs. The model extends to the stack level, with realistic penalties placed on usable capacity, overpotential, excess lithium/electrolyte, and most importantly active material mass fraction. A full description of the assumptions and calculations made herein is given in the supplementary information.

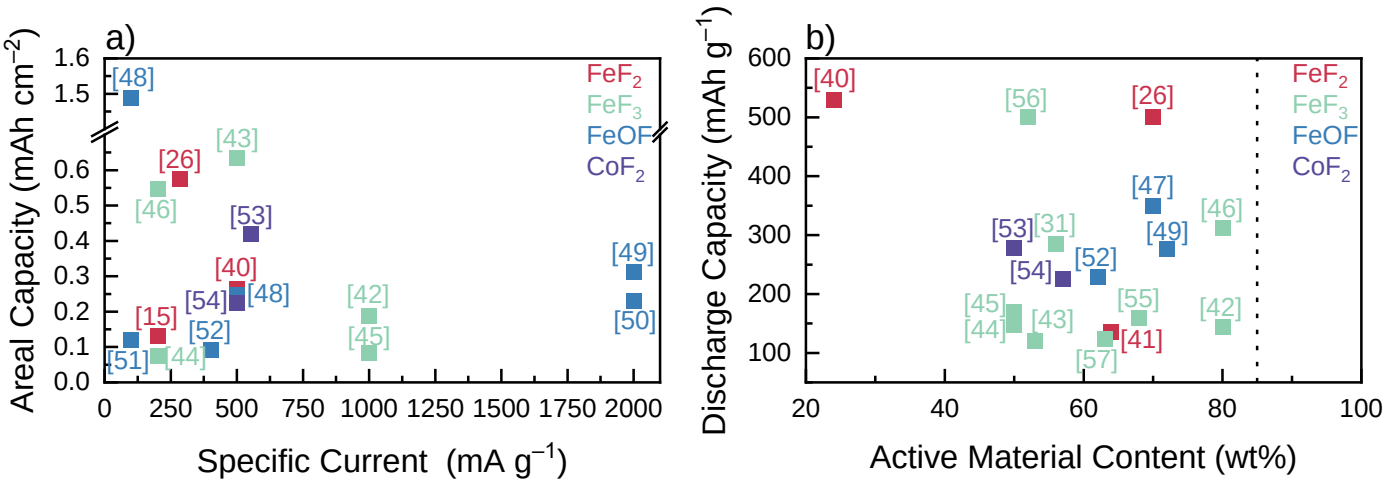

Figure 3: High rate performance comparison of various TMF cathodes.[33, 40, 26, 28, 15, 41, 42, 31, 43, 44, 45, 46, 47, 48, 49, 50, 51, 52, 53, 54, 55, 56, 57] **a** shows the areal capacity obtained at a given current density and **b** the corresponding discharge capacities as a function of active material content in the cathode. The dotted line indicates the threshold of 85 wt% used for the techno-economic calculation. Noteworthy, not every publication reports enough information to calculate both the areal capacity and active material content. The colors indicate elements used in the cathode.

It is more pertinent to compare TMF chemistries with a hypothetical $LiNi_{0.8}Co_{0.1}Mn_{0.1}O_2$ (NMC_{811}) lithium system, as both cases depend on a lithium metal anode. While all the TMF systems considered here exhibit higher energy densities, it is questionable whether the modest advantage (50 W h kg^{-1} to 70 W h kg^{-1} increase compared to NMC_{811}-lithium) of the lower potential cathodes (FeF_2, CoF_2) could justify the use of a chemistry with inferior cycle life and rate capability (Figure 4a). The increase in cathode potential from FeF_2 to CuF_2 yields a drastic increase in energy density, highlighting the importance of incorporating more electronegative transition metals and decreasing discharge overpotentials (<300 mV). NiF_2, CuF_2, FeF_3 systems could exceed 600 W h kg^{-1} at the stack level, with potential for use in high specific energy applications. Additionally CuF_2 and FeF_3 are highly competitive in terms of cost of energy stored (US $ per kWh), with the main cost drivers being the lithium anode and electrolyte Figure 4b.

Despite the obvious theoretical advantages of iron (III) fluoride over the divalent compound (higher redox potential and larger specific capacity), intrinsic kinetic limitations undermine its practical implementation. As a result of the higher LiF concentration in a converted FeF_3 compound (3 LiF per Fe^0), reaction kinetics are intrinsically more sluggish compared to FeF_2 (2 LiF per Fe^0) thus negatively affecting rate capability. [29] To the best of our knowledge, a reversible capacity retention corresponding to all three Li equivalents (712 mA h g^{-1}) has not been demonstrated for more than ten cycles yet. [56] While capacity loss induced by isolation of iron particles in a FeF_2 compound can be compensated by oxidation of other metal centres beyond Fe^{2+}, this is not possible in FeF_3. [26]

Albeit CuF_2 holds the greatest potential value, it is the only 3d TMF cathode that shows little to no intrinsic reversibility. Despite its structural similarities (CuF_2 exhibits a monoclinic structure, which is Jahn-Teller distorted from the typical tetragonal rutile of other transition metal difluorides), CuF_2 cycling exhibits poor reversibility, which restricted its application to primary batteries so far. [10, 60, 61] Studies have suggested that metallic copper does not nucleate inside the fluoride sublattice on discharge but instead forms large aggregates on the particle surface due to the high diffusivity of copper cations. [17, 61] During charge, substantial copper dissolution by the formation of fluoride rich complex ions, such as $[Cu^{I}F_4]^{3-}$ and $[Cu^{II}F_6]^{4-}$, associated with the consumption of LiF is observed. [62]

Promising results were published by Wang *et al.*, who reported reversible Cu redox reaction over a two-step reduction in a $Cu_yFe_{1-y}F_2$ solid-solution compound. [63] An unprecedentedly low voltage hysteresis (<150 mV in galvanostatic intermittent titration technique, GITT) was observed, which suggested ternary compounds as an avenue for overcoming low energy efficiencies characteristic of TMF cathodes. [23] However, more recent publications have tempered this enthusiasm.

Gordon *et al.* investigated a number of solid-solution ternary difluoride (Fe-Co, Fe-Mn, Fe-Ni) nanoparticles decorating multi-wall carbon nanotubes (MWCNT). [64] In contrast to Wang *et al.* the authors did not observe any mitigation of the voltage hysteresis compared to plain FeF_2. Additionally, mixed metal reduction appeared to occur in a single step reaction and the average discharge potentials lied in between the ones corresponding to the binary fluorides. Although this does suggest a certain degree of tunability, it should be noted that all of the ternary fluorides exhibited lower average discharge potentials compared to FeF_2. On the contrary, substituting copper into a nickel fluoride compound is reported to increase the discharge

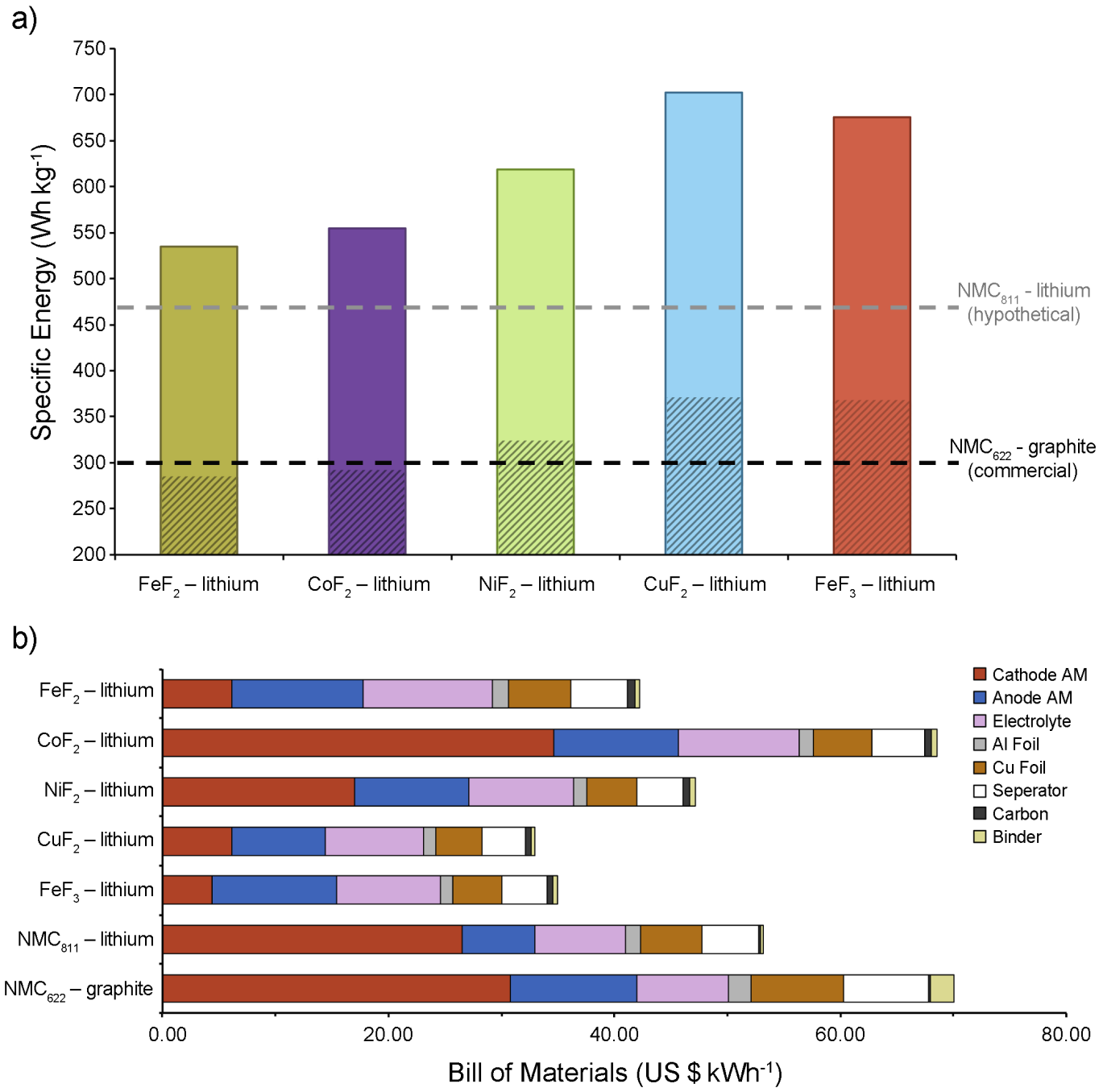

Figure 4: Techno-econmic analysis of TMF chemistries. a, Chart showing the projected specific energy at the stack level for the later 3d transition metal fluoride cathodes with lithium metal anodes. These values were calculated for 90 µm thick cathodes with 30% porosity, assuming 85% active material mass fraction, a usable capacity at 90% of the theoretical, an average cathode overpotential of 300 mV, 30% excess lithium capacity, and 150% excess electrolyte mass as realistically achievable parameters. The textured regions of the chart represent a drop in active material mass fraction from 85% to 50%. The grey and black dashed lines represents the stack level specific energy of a commercial scale $LiNi_{0.6}Mn_{0.2}Co_{0.2}O_2$ (NMC_{622}) graphite cell and a hypothetical $LiNi_{0.8}Co_{0.1}Mn_{0.1}O_2$ (NMC_{811}) lithium cell respectively. These cells are modeled for high-energy with a maximum electrode thickness of 90 µm, containing 96-98% active material at 25-30% porosity. A number of parameters used in this model were obtained from the Battery Performance and Cost (BatPaC) modelling software developed by Argonne National Laboratory. A detailed description of the technoeconomic model is provided in the supplementary information. **b**, Chart describing the bill of materials as a fractions of the total cost of energy stored for five transition metal fluoride-lithium cell chemistries as well as high-energy NMC_{622}-graphite and NMC_{811}-lithium cells. The prices of transition metal fluoride active materials were estimated from the most recent (late 2020) spot prices of the commodity chemicals used in their synthesis, with rough approximations for the cost of production as detailed in the Supplementary Information.

potential by a few hundred millivolts. [65] Interestingly, further oxidation of some metal centers to a +3 state of charge in Mn and Fe containing compounds was indicated in their voltage profiles. [64]

A similar observation was made by Omenya *et al.* The group showed fairly reversible cycling in a $Cu_{0.5}Fe_{0.5}F_2$ compound. However, X-ray absorption near edge structure (XANES) measurements suggested that only a small amount of copper is re-oxidized during charge. Instead, reversible oxidation beyond Fe^{2+} compensates for capacity loss due to copper isolation and dissolution into the electrolyte. [61] In addition, a significantly higher hysteresis was monitored by potentiostatic intermittent titration technique (PITT) compared to the GITT data from Wang *et al.* It is reported that GITT does not monitor certain overpotentials in conversion materials and thus can exhibit a lower voltage hysteresis. [29]

To address the problem of copper dissolution, Seo *et al.* prepared a NiO protection layer on a CuF_2/C electrode. In contrast to a bare CuF_2/C composite the cathode could be recharged and five subsequent cycles are demonstrated. Inductively coupled plasma optical emission spectroscopy (ICP-OES) of the electrolyte indicated a substantial alleviation of copper dissolution by the NiO coating. [66] Nevertheless, significant capacity fading is observed, indicating the existence of vast overpotentials for the reconversion of CuF_2. A further investigation of the interfaces formed between metallic Cu and CuF_2/LiF may help to explain the origin of this anomalous behavior.

In addition to mixed cation TMFs, mixed anion oxyfluoride compounds (formed by substituting O^{2-} at the F^- lattice site) have also demonstrated improved performance in the past. [67, 68, 29] A recent publication by Fan *et al.* reported co-substituted $Fe_{0.9}Co_{0.1}OF$ nanorods. In contrast to the pristine phases (FeOF, FeF_3), the compound showed remarkable cycling stability, retaining 350 mA h g^{-1} for over 1000 cycles which corresponds to a capacity fade of 0.005% per cycle. As evident from GITT, the potential hysteresis could be significantly reduced down to 0.27 V at 50% SOC compared to FeOF (0.57 V) and FeF_3 (1.1 V). Supported by first principle calculations the authors rationalize the outstanding electrochemical performance by suppressing the conversion reaction due to concerted Co/O doping. An intercalation-extrusion mechanism is enabled by stabilizing a defected-rocksalt parent phase ($Li_{1-0.5z}Fe(Co)O_{2-z}$), where only small amounts of metallic Fe(Co) is formed (extruded) and a high lattice coherence with LiF is maintained. [47] The study is a pioneering example of how co-substitution can be used to modify the reaction mechanism and thus tune the electrochemical performance of TMF cathodes.

5. The Future of Conversion-Type Fluoride Cathodes

Within the last couple of years, transition metal fluoride cathodes have proven themselves promising candidates for the next generation of energy dense cathode materials. Recent publications have shown how the cycling stability of FeF_x can be significantly improved by choosing an adequate electrolyte composition. By elucidating the role of a stable parent phase throughout cycling, the common misconception of inherently sluggish reaction kinetics in FeF_x cathodes were proven wrong. Rational design of such phases resulted in remarkable capacity retention. At this stage, the commercial utility of TMF cathodes will determined by the achievable active material mass fraction and areal capacity loading. Increasing the active material mass fraction of TMF cathodes toward 85% will be necessary for development of a commercially competitive technology. An active material loading between 2 mg cm^{-2} to 3 mg cm^{-2} should be maintained in future publications to facilitate the comparison of results and evaluate the commercial viability of potential strategies for performance improvement. In our experience, such loadings are achievable at the lab-scale and would produce an areal capacity comparable to lower energy commercial cells, for example, 3 mg cm^{-2} of FeF_2 would have the same areal capacity as 8 mg cm^{-2} of NMC_{622} ($\sim$1.5 mA h cm^{-2}). Although further increases in mass loading will be required to surpass the areal capacities of current LIBs, cells built at this intermediate scale will allow a more meaningful evaluation of performance. Recently, a wealth of mechanistic understanding has been generated for the FeF_x system, in the pursuit of more useful information further mechanistic studies should instead focus on higher energy systems. While reversible cycling of pure CuF_2 has proven problematic, the possibility of increasing cathode potential through Cu cation substitution should not be ignored.

Acknowledgements

This work was supported by funding from the Engineering and Physical Sciences Research Council (grant number EP/R511742/1), the Henry Royce Institute for capital equipment (through UK Engineering and Physical Science Research Council grant EP/R010145/1) and by the Army Research Office (ARO) (grant number W911NF-20-1-0210). The views and conclusions contained in this document are those of the authors and should not be interpreted as representing the official policies, either expressed or implied, of ARO or the U.S. Government. The U.S. Government is authorized to reproduce and distribute reprints for Government purposes notwithstanding any copyright notation herein. The authors would like to thank Jack Fawdon for insightful conversations and constructive comments.

Conflicts of interest

There are no conflicts to declare.

References

[1] IEA, Global EV Outlook 2020 – Analysis - IEA (2020).
URL https://www.iea.org/reports/global-ev-outlook-2020

[2] J. Janek, W. G. Zeier, A solid future for battery development, Nature Energy 1 (9) (2016) 1–4. doi:10.1038/nenergy.2016.141.
URL http://dx.doi.org/10.1038/nenergy.2016.141

[3] A. W. Schäfer, S. R. Barrett, K. Doyme, L. M. Dray, A. R. Gnadt, R. Self, A. O'Sullivan, A. P. Synodinos, A. J. Torija, Technological, economic and environmental prospects of all-electric aircraft, Nature Energy 4 (2) (2019) 160–166. doi:10.1038/s41560-018-0294-x.
URL http://dx.doi.org/10.1038/s41560-018-0294-x

[4] L. Wang, Z. Wu, J. Zou, P. Gao, X. Niu, H. Li, L. Chen, Li-free Cathode Materials for High Energy Density Lithium Batteries, Joule 3 (9) (2019) 2086–2102. doi:10.1016/j.joule.2019.07.011.
URL https://doi.org/10.1016/j.joule.2019.07.011

[5] F. Wu, J. Maier, Y. Yu, Guidelines and trends for next-generation rechargeable lithium and lithium-ion batteries, Chemical Society Reviews 49 (5) (2020) 1569–1614. doi:10.1039/c7cs00863e.

[6] F. Wu, G. Yushin, Conversion cathodes for rechargeable lithium and lithium-ion batteries, Energy and Environmental Science 10 (2) (2017) 435–459. doi:10.1039/c6ee02326f.

[7] F. Badway, F. Cosandey, N. Pereira, G. G. Amatucci, Carbon Metal Fluoride Nanocomposites, Journal of The Electrochemical Society 150 (10) (2003) A1318. doi:10.1149/1.1602454.

[8] F. Badway, N. Pereira, F. Cosandey, G. G. Amatucci, Carbon-Metal Fluoride Nanocomposites, Journal of The Electrochemical Society 150 (9) (2003) A1209. doi:10.1149/1.1596162.

[9] H. Li, G. Richter, J. Maier, Reversible formation and decomposition of LiF clusters using transition metal fluorides as precursors and their application in rechargeable Li batteries, Advanced Materials 15 (9) (2003) 736–739. doi:10.1002/adma.200304574.

[10] F. Badway, A. N. Mansour, N. Pereira, J. F. Al-Sharab, F. Cosandey, I. Plitz, G. G. Amatucci, Structure and electrochemistry of copper fluoride nanocomposites utilizing mixed conducting matrices, Chemistry of Materials 19 (17) (2007) 4129–4141. doi:10.1021/cm070421g.

[11] L. Liu, M. Zhou, L. Yi, H. Guo, J. Tan, H. Shu, X. Yang, Z. Yang, X. Wang, Excellent cycle performance of Co-doped FeF 3/C nanocomposite cathode material for lithium-ion batteries, Journal of Materials Chemistry 22 (34) (2012) 17539–17550. doi:10.1039/c2jm32936k.

[12] M. A. Reddy, B. Breitung, V. S. K. Chakravadhanula, C. Wall, M. Engel, C. Kübel, A. K. Powell, H. Hahn, M. Fichtner, CFx derived carbon-FeF2nanocomposites for reversible lithium storage, Advanced Energy Materials 3 (3) (2013) 308–313. doi:10.1002/aenm.201200788.

[13] J. Zhou, D. Zhang, X. Zhang, H. Song, X. Chen, Carbon-nanotube-encapsulated FeF2 nanorods for high-performance lithium-ion cathode materials, ACS Applied Materials and Interfaces 6 (23) (2014) 21223–21229. doi:10.1021/am506236n.

[14] X. Fan, Y. Zhu, C. Luo, L. Suo, Y. Lin, T. Gao, K. Xu, C. Wang, Pomegranate-Structured Conversion-Reaction Cathode with a Built-in Li Source for High-Energy Li-Ion Batteries, ACS Nano 10 (5) (2016) 5567–5577. doi:10.1021/acsnano.6b02309.

[15] S. Kim, J. Liu, K. Sun, J. Wang, S. J. Dillon, P. V. Braun, Improved Performance in FeF2 Conversion Cathodes through Use of a Conductive 3D Scaffold and Al2O3 ALD Coating, Advanced Functional Materials 27 (35) (2017) 1–8. doi:10.1002/adfm.201702783.

[16] R. E. Doe, K. A. Persson, Y. S. Meng, G. Ceder, First-principles investigation of the Li-Fe-F phase diagram and equilibrium and nonequilibrium conversion reactions of iron fluorides with lithium, Chemistry of Materials 20 (16) (2008) 5274–5283. doi:10.1021/cm801105p.

[17] F. Wang, R. Robert, N. A. Chernova, N. Pereira, F. Omenya, F. Badway, X. Hua, M. Ruotolo, R. Zhang, L. Wu, V. Volkov, D. Su, B. Key, M. Stanley Whittingham, C. P. Grey, G. G. Amatucci, Y. Zhu, J. Graetz, Conversion reaction mechanisms in lithium ion batteries: Study of the binary metal fluoride electrodes, Journal of the American Chemical Society 133 (46) (2011) 18828–18836. doi:10.1021/ja206268a.

[18] F. Wang, H. C. Yu, M. H. Chen, L. Wu, N. Pereira, K. Thornton, A. Van Der Ven, Y. Zhu, G. G. Amatucci, J. Graetz, Tracking lithium transport and electrochemical reactions in nanoparticles, Nature Communications 3 (2012) 1201–1208. doi:10.1038/ncomms2185.
URL http://dx.doi.org/10.1038/ncomms2185

[19] C. Li, L. Gu, J. Maier, Enhancement of the Li conductivity in LiF by introducing glass/crystal interfaces, Advanced Functional Materials 22 (6) (2012) 1145–1149. doi:10.1002/adfm.201101798.

[20] Y. Ma, S. H. Garofalini, Atomistic insights into the conversion reaction in iron fluoride: A dynamically adaptive force field approach, Journal of the American Chemical Society 134 (19) (2012) 8205–8211. doi:10.1021/ja301637c.

[21] Y. Ma, S. H. Garofalini, Interplay between the ionic and electronic transport and its effects on the reaction pattern during the electrochemical conversion in an FeF2 nanoparticle, Physical Chemistry Chemical Physics 16 (23) (2014) 11690–11697. doi:10.1039/c4cp00481g.

[22] L. Li, Y. C. K. Chen-Wiegart, J. Wang, P. Gao, Q. Ding, Y. S. Yu, F. Wang, J. Cabana, J. Wang, S. Jin, Visualization of electrochemically driven solid-state phase transformations using operando hard X-ray spectro-imaging, Nature Communications 6 (2015) 1–8. doi:10.1038/ncomms7883.

[23] L. Li, R. Jacobs, P. Gao, L. Gan, F. Wang, D. Morgan, S. Jin, Origins of Large Voltage Hysteresis in High-Energy-Density Metal Fluoride Lithium-Ion Battery Conversion Electrodes, Journal of the American Chemical Society 138 (8) (2016) 2838–2848. doi:10.1021/jacs.6b00061.

[24] C. Li, K. Chen, X. Zhou, J. Maier, Electrochemically driven conversion reaction in fluoride electrodes for energy storage devices, npj Computational Materials 4 (1) (2018). doi:10.1038/s41524-018-0079-6.
URL http://dx.doi.org/10.1038/s41524-018-0079-6

[25] K. Karki, L. Wu, Y. Ma, M. J. Armstrong, J. D. Holmes, S. H. Garofalini, Y. Zhu, E. A. Stach, F. Wang, Revisiting Conversion Reaction Mechanisms in Lithium Batteries: Lithiation-Driven Topotactic Transformation in FeF 2, Journal of the American Chemical Society 140 (51) (2018) 17915–17922. doi:10.1021/jacs.8b07740.

[26] A. W. Xiao, H. J. Lee, I. Capone, A. Robertson, T. U. Wi, J. Fawdon, S. Wheeler, H. W. Lee, N. Grobert, M. Pasta, Understanding the conversion mechanism and performance of monodisperse FeF2 nanocrystal cathodes, Nature Materials 19 (6) (2020) 644–654. doi:10.1038/s41563-020-0621-z.
URL http://dx.doi.org/10.1038/s41563-020-0621-z

[27] X. Hua, A. S. Eggeman, E. Castillo-Martínez, R. Robert, H. S. Geddes, Z. Lu, C. J. Pickard, W. Meng, K. M. Wiaderek, N. Pereira, G. G. Amatucci, P. A. Midgley, K. W. Chapman, U. Steiner, A. L. Goodwin, C. P. Grey, Revisiting metal fluorides as lithium-ion battery cathodes, Nature Materials (1 2021). doi:10.1038/s41563-020-00893-1.
URL http://www.nature.com/articles/s41563-020-00893-1

[28] Q. Huang, K. Turcheniuk, X. Ren, A. Magasinski, D. Gordon, N. Bensalah, G. Yushin, Insights into the Effects of Electrolyte Composition on the Performance and Stability of FeF 2 Conversion-Type Cathodes, Advanced Energy Materials 9 (17) (2019) 1–11. doi:10.1002/aenm.201803323.

[29] J. K. Ko, K. M. Wiaderek, N. Pereira, T. L. Kinnibrugh, J. R. Kim, P. J. Chupas, K. W. Chapman, G. G. Amatucci, Transport, phase reactions, and hysteresis of iron fluoride and oxyfluoride conversion electrode materials for lithium batteries, ACS Applied Materials and Interfaces 6 (14) (2014) 10858–10869. doi:10.1021/am500538b.

[30] W. Gu, O. Borodin, B. Zdyrko, H. T. Lin, H. Kim, N. Nitta, J. Huang, A. Magasinski, Z. Milicev, G. Berdichevsky, G. Yushin, Lithium-Iron Fluoride Battery with in Situ Sur-

face Protection, Advanced Functional Materials 26 (10) (2016) 1507–1516. doi:10.1002/adfm.201504848.

[31] W. Fu, E. Zhao, Z. Sun, X. Ren, A. Magasinski, G. Yushin, Iron Fluoride–Carbon Nanocomposite Nanofibers as Free-Standing Cathodes for High-Energy Lithium Batteries, Advanced Functional Materials 28 (32) (2018) 1–8. doi:10.1002/adfm.201801711.

[32] E. Zhao, O. Borodin, X. Gao, D. Lei, Y. Xiao, X. Ren, W. Fu, A. Magasinski, K. Turcheniuk, G. Yushin, Lithium–Iron (III) Fluoride Battery with Double Surface Protection, Advanced Energy Materials 8 (26) (2018) 1–11. doi:10.1002/aenm.201800721.

[33] Q. Huang, K. Turcheniuk, X. Ren, A. Magasinski, A. Y. Song, Y. Xiao, D. Kim, G. Yushin, Cycle stability of conversion-type iron fluoride lithium battery cathode at elevated temperatures in polymer electrolyte composites, Nature Materials 18 (12) (2019) 1343–1349. doi:10.1038/s41563-019-0472-7.
URL http://dx.doi.org/10.1038/s41563-019-0472-7

[34] I. A. Shkrob, T. W. Marin, Y. Zhu, D. P. Abraham, Why bis(fluorosulfonyl)imide is a "magic anion" for electrochemistry, Journal of Physical Chemistry C 118 (34) (2014) 19661–19671. doi:10.1021/jp506567p.

[35] T. Li, X. Q. Zhang, P. Shi, Q. Zhang, Fluorinated Solid-Electrolyte Interphase in High-Voltage Lithium Metal Batteries, Joule 3 (11) (2019) 2647–2661. doi:10.1016/j.joule.2019.09.022.
URL https://doi.org/10.1016/j.joule.2019.09.022

[36] X. Ren, P. Gao, L. Zou, S. Jiao, X. Cao, X. Zhang, H. Jia, M. H. Engelhard, B. E. Matthews, H. Wu, H. Lee, C. Niu, C. Wang, B. W. Arey, J. Xiao, J. Liu, J. G. Zhang, W. Xu, Role of inner solvation sheath within salt–solvent complexes in tailoring electrode/electrolyte interphases for lithium metal batteries, Proceedings of the National Academy of Sciences of the United States of America 117 (46) (2020) 28603–28613. doi:10.1073/pnas.2010852117.

[37] J. Wang, Y. Yamada, K. Sodeyama, C. H. Chiang, Y. Tateyama, A. Yamada, Superconcentrated electrolytes for a high-voltage lithium-ion battery, Nature Communications 7 (May) (2016) 1–9. doi:10.1038/ncomms12032.

[38] Y. Yamada, J. Wang, S. Ko, E. Watanabe, A. Yamada, Advances and issues in developing salt-concentrated battery electrolytes, Nature Energy 4 (4) (2019) 269–280. doi:10.1038/s41560-019-0336-z.
URL http://dx.doi.org/10.1038/s41560-019-0336-z

[39] Z. Yu, H. Wang, X. Kong, W. Huang, Y. Tsao, D. G. Mackanic, K. Wang, X. Wang, W. Huang, S. Choudhury, Y. Zheng, C. V. Amanchukwu, S. T. Hung, Y. Ma, E. G. Lomeli, J. Qin, Y. Cui, Z. Bao, Molecular design for electrolyte solvents enabling energy-dense and long-cycling lithium metal batteries, Nature Energy 5 (7) (2020) 526–533. doi:10.1038/s41560-020-0634-5.
URL http://dx.doi.org/10.1038/s41560-020-0634-5

[40] H. Song, H. Cui, C. Wang, Extremely high-rate capacity and stable cycling of a highly ordered nanostructured carbon-FeF2 battery cathode, Journal of Materials Chemistry A 3 (44) (2015) 22377–22384. doi:10.1039/c5ta06297g.
URL http://dx.doi.org/10.1039/C5TA06297G

[41] W. Gu, A. Magasinski, B. Zdyrko, G. Yushin, Metal fluorides nanoconfined in carbon nanopores as reversible high capacity cathodes for Li and Li-Ion rechargeable batteries: FeF2 as an example, Advanced Energy Materials 5 (4) (2015) 1–7. doi:10.1002/aenm.201401148.

[42] Y. Han, H. Li, J. Li, H. Si, W. Zhu, X. Qiu, Hierarchical Mesoporous Iron Fluoride with Superior Rate Performance for Lithium-Ion Batteries, ACS Applied Materials and Interfaces 8 (48) (2016) 32869–32874. doi:10.1021/acsami.6b11889.

[43] F. Wu, V. Srot, S. Chen, S. Lorger, P. A. van Aken, J. Maier, Y. Yu, 3D Honeycomb Architecture Enables a High-Rate and Long-Life Iron (III) Fluoride–Lithium Battery, Advanced Materials 31 (43) (2019) 1–9. doi:10.1002/adma.201905146.

[44] Q. Zhang, Y. Zhang, Y. Yin, L. Fan, N. Zhang, Packing FeF3 · 0.33H2O into porous graphene/carbon nanotube network as high volumetric performance cathode for lithium ion battery, Journal of Power Sources 447 (August 2019) (2020) 227303. doi:10.1016/j.jpowsour.2019.227303.
URL https://doi.org/10.1016/j.jpowsour.2019.227303

[45] C. P. Guntlin, T. Zünd, K. V. Kravchyk, M. Wörle, M. I. Bodnarchuk, M. V. Kovalenko, Nanocrystalline FeF3 and MF2 (M = Fe, Co, and Mn) from metal trifluoroacetates and their Li(Na)-ion storage properties, Journal of Materials Chemistry A 5 (16) (2017) 7383–7393. doi:10.1039/c7ta00862g.

[46] M. Liu, Q. Wang, B. Chen, H. Lei, L. Liu, C. Wu, X. Wang, Z. Yang, Band-Gap Engineering of FeF3 · 0.33H2O Nanosphere via Ni Doping as a High-Performance Lithium-Ion Battery Cathode, ACS Sustainable Chemistry and Engineering 8 (41) (2020) 15651–15660. doi:10.1021/acssuschemeng.0c05258.

[47] X. Fan, E. Hu, X. Ji, Y. Zhu, F. Han, S. Hwang, J. Liu, S. Bak, Z. Ma, T. Gao, S. C. Liou, J. Bai, X. Q. Yang, Y. Mo, K. Xu, D. Su, C. Wang, High energy-density and reversibility of iron fluoride cathode enabled via an intercalation-extrusion reaction, Nature Communications 9 (1) (2018) 1–12. doi:10.1038/s41467-018-04476-2.
URL http://dx.doi.org/10.1038/s41467-018-04476-2

[48] W. Li, Y. Chen, A. Zangiabadi, Z. Li, X. Xiao, W. Huang, Q. Cheng, S. Lou, H. Zhang, A. Cao, X. Roy, Y. Yang, FeOF/TiO2Hetero-Nanostructures for High-Areal-Capacity Fluoride Cathodes, ACS Applied Materials and Interfaces 12 (30) (2020) 33803–33809. doi:10.1021/acsami.0c09185.

[49] J. Zhai, Z. Lei, K. Sun, 3D Starfish-Like FeOF on Graphene Sheets: Engineered Synthesis and Lithium Storage Performance, Chemistry - A European Journal 25 (32) (2019) 7733–7739. doi:10.1002/chem.201900948.

[50] X. Li, Y. Zhang, Y. Meng, Y. Wang, G. Tan, H. Yuan, D. Xiao, Three-dimensional iron oxyfluoride/N-doped carbon hybrid nanocomposites as high-performance cathodes for rechargeable Li-ion batteries, Inorganic Chemistry Frontiers 6 (2) (2019) 465–472. doi:10.1039/c8qi01057a.

[51] L. Ju, G. Wang, K. Liang, M. Wang, G. E. Sterbinsky, Z. Feng, Y. Yang, Significantly Improved Cyclability of Conversion-Type Transition Metal Oxyfluoride Cathodes by Homologous Passivation Layer Reconstruction, Advanced Energy Materials 10 (9) (2020) 1–8. doi:10.1002/aenm.201903333.

[52] X. Fan, C. Luo, J. Lamb, Y. Zhu, K. Xu, C. Wang, PEDOT Encapsulated FeOF Nanorod Cathodes for High Energy Lithium-Ion Batteries, Nano Letters 15 (11) (2015) 7650–7656. doi:10.1021/acs.nanolett.5b03601.

[53] F. Wu, V. Srot, S. Chen, M. Zhang, P. A. Van Aken, Y. Wang, J. Maier, Y. Yu, Metal-Organic Framework-Derived Nanoconfinements of CoF2and Mixed-Conducting Wiring for High-Performance Metal Fluoride-Lithium Battery, ACS Nano (2021). doi:10.1021/acsnano.0c08918.

[54] X. Wang, W. Gu, J. T. Lee, N. Nitta, J. Benson, A. Magasinski, M. W. Schauer, G. Yushin, Carbon Nanotube-CoF2 Multifunctional Cathode for Lithium Ion Batteries: Effect of Electrolyte on Cycle Stability, Small 11 (38) (2015) 5164–5173. doi:10.1002/smll.201501139.

[55] J. Tan, L. Liu, H. Hu, Z. Yang, H. Guo, Q. Wei, X. Yi, Z. Yan, Q. Zhou, Z. Huang, H. Shu, X. Yang, X. Wang, Iron fluoride with excellent cycle performance synthesized by solvothermal method as cathodes for lithium ion batteries, Journal of Power Sources 251 (2014) 75–84. doi:10.1016/j.jpowsour.2013.11.004.
URL http://dx.doi.org/10.1016/j.jpowsour.2013.11.004

[56] T. Li, L. Li, Y. L. Cao, X. P. Ai, H. X. Yang, Reversible three-electron redox behaviors of FeF3 nanocrystals as high-capacity cathode-active materials for Li-Ion batteries, Journal of Physical Chemistry C 114 (7) (2010) 3190–3195. doi:10.1021/jp908741d.

[57] Q. Chu, Z. Xing, X. Ren, A. M. Asiri, A. O. Al-Youbi, K. A. Alamry, X. Sun, Reduced graphene oxide decorated with FeF3 nanoparticles: Facile synthesis and application as a high capac-

ity cathode material for rechargeable lithium batteries, Electrochimica Acta 111 (2013) 80–85. doi:10.1016/j.electacta.2013.08.006.
URL http://dx.doi.org/10.1016/j.electacta.2013.08.006

[58] M. Tang, Z. Zhang, Z. Wang, J. Liu, H. Yan, J. Peng, High-Temperature Electrochemical Performance of FeF3/C Nanocomposite as a Cathode Material for Lithium-Ion Batteries, Journal of Materials Engineering and Performance 27 (2) (2018) 624–629. doi:10.1007/s11665-018-3167-3.
URL https://doi.org/10.1007/s11665-018-3167-3

[59] Y. Zheng, S. Tawa, J. Hwang, Y. Orikasa, K. Matsumoto, R. Hagiwara, Phase Evolution of Trirutile Li 0 . 5 FeF 3 for Lithium-Ion Batteries (2021). doi:10.1021/acs.chemmater.0c03544.

[60] F. Badway, N. Brunswick, R. U. S. A. Data, (12) United States Patent 2 (12) (2015).

[61] F. Omenya, N. J. Zagarella, J. Rana, H. Zhang, C. Siu, H. Zhou, B. Wen, N. A. Chernova, L. F. Piper, G. Zhou, M. S. Whittingham, Intrinsic Challenges to the Electrochemical Reversibility of the High Energy Density Copper(II) Fluoride Cathode Material, ACS Applied Energy Materials 2 (7) (2019) 5243–5253. doi:10.1021/acsaem.9b00938.

[62] X. Hua, R. Robert, L. S. Du, K. M. Wiaderek, M. Leskes, K. W. Chapman, P. J. Chupas, C. P. Grey, Comprehensive study of the CuF2 conversion reaction mechanism in a lithium ion battery, Journal of Physical Chemistry C 118 (28) (2014) 15169–15184. doi:10.1021/jp503902z.

[63] F. Wang, S. W. Kim, D. H. Seo, K. Kang, L. Wang, D. Su, J. J. Vajo, J. Wang, J. Graetz, Ternary metal fluorides as high-energy cathodes with low cycling hysteresis, Nature Communications 6 (2015) 1–9. doi:10.1038/ncomms7668.
URL http://dx.doi.org/10.1038/ncomms7668

[64] D. Gordon, Q. Huang, A. Magasinski, A. Ramanujapuram, N. Bensalah, G. Yushin, Mixed Metal Difluorides as High Capacity Conversion-Type Cathodes: Impact of Composition on Stability and Performance, Advanced Energy Materials 8 (19) (2018) 1–10. doi:10.1002/aenm.201800213.

[65] C. Villa, S. Kim, Y. Lu, V. P. Dravid, J. Wu, Cu-Substituted NiF 2 as a Cathode Material for Li-Ion Batteries, ACS Applied Materials and Interfaces 11 (1) (2019) 647–654. doi:10.1021/acsami.8b15791.

[66] J. K. Seo, H. M. Cho, K. Takahara, K. W. Chapman, O. J. Borkiewicz, M. Sina, Y. Shirley Meng, Revisiting the conversion reaction voltage and the reversibility of the CuF2 electrode in Li-ion batteries, Nano Research 10 (12) (2017) 4232–4244. doi:10.1007/s12274-016-1365-6.

[67] N. Pereira, F. Badway, M. Wartelsky, S. Gunn, G. G. Amatucci, Iron Oxyfluorides as High Capacity Cathode Materials for Lithium Batteries, Journal of The Electrochemical Society 156 (6) (2009) A407. doi:10.1149/1.3106132.

[68] S. W. Kim, N. Pereira, N. A. Chernova, F. Omenya, P. Gao, M. S. Whittingham, G. G. Amatucci, D. Su, F. Wang, Structure Stabilization by Mixed Anions in Oxyfluoride Cathodes for High-Energy Lithium Batteries, ACS Nano 9 (10) (2015) 10076–10084. doi:10.1021/acsnano.5b03643.